

# Recent Progress Towards a High-Speed Three-Dimensional Flow Visualization Technique

B. S. Thurow

Auburn University, Dept. of Aerospace Engineering  
211 Aerospace Engineering Bldg.  
Auburn, AL 36849  
(334) 844-6827  
[thurow@auburn.edu](mailto:thurow@auburn.edu)

**Advances in high-repetition rate laser and camera technology present a renewed opportunity to develop high-speed three-dimensional flow diagnostics based on the rapid scanning of a laser sheet through a flow field. Recent progress towards developing a high-speed 3-D flow visualization system is presented. The system is based on a MHz rate pulse burst laser, a galvanometric scanning mirror and an ultra-high-speed camera. Once development is complete, the system will be able to acquire a 3-D image in tens of microseconds, making it suitable for a broad range of high-speed flow fields. In this paper, a low-speed version of the system was used to image the 3-D structure of vortex rings emitted from a small smoke chamber. The rich nature of the 3-D images demonstrates the inherent potential of the technique. Future work includes incorporation of the pulse burst laser into the 3-D system.**

## I. INTRODUCTION

Numerous efforts have been made over the years to develop 3-D flow measurement systems. These include stereographic [1], holographic [2-4], tomographic [5], and laser scanning [6-15] methods. The approach that has received the most attention and is adopted in this effort is that of laser scanning. In this technique, a laser beam, formed into a sheet using cylindrical lenses, is scanned through the flow field using an optical deflector, such as a rotating mirror. As the laser sheet passes through the flow field, a sequence of images, each corresponding to a different plane in the flow field, is acquired. A 3-D image is then reconstructed from the sequence of images. A significant advantage to this method is that it inherently utilizes many of the measurement concepts and principles already developed for conventional planar techniques, such as particle image velocimetry (PIV) and planar laser induced fluorescence (PLIF). Thus, extension of these techniques to 3-D can be rather straightforward. For the most part, however, the application of 3-D diagnostics based on laser scanning has been restricted to low-speed flows ( $V < 1$  m/s) due to the limited repetition rate of available lasers, cameras and scanning mirrors.

Past efforts to develop high-speed 3-D imaging techniques, such as those by Refs. [7, 8, 9, 11 & 14] have demonstrated the potential of high-speed 3-D imaging. Broad application of these techniques, however, has not been realized due to the

limited capabilities and expense of the specialized equipment necessary for their implementation. Recent advances in high-repetition rate laser and camera technology, however, have greatly improved upon the capabilities and availability of this equipment. For example, there are now over a dozen manufacturers that offer cameras with framing rates of 1,000,000 fps or greater. These advances present a renewed opportunity to develop 3-D laser scanning flow diagnostics that have the potential to be applied in a much greater number of laboratories.

The Advanced Laser Diagnostics Laboratory (ALDL) at Auburn University has recently launched an effort to develop a high-speed laser-scanning 3-D flow visualization system. It is based on a 3rd generation MHz rate pulse burst laser system, a commercially available high-speed camera and a high-speed galvanometric scanning mirror. This paper describes recent progress in efforts to develop this system and presents recent results obtained using a low-speed version of the system. The long-term goal of the work is to develop a high-speed system capable of acquiring a complete 3-D image in tens of microseconds.

## II. HIGH-SPEED 3-D IMAGING CONCEPT

A general schematic of the 3-D imaging system being developed at the ALDL is shown in Figure 1. The system is based on three core components: a pulse burst laser system, a high speed galvanometric scanning mirror, and an ultra-high speed camera. Pulses from the pulse burst laser, separated by as little as 1 microsecond or less each, are deflected along different paths using a galvanometric scanning mirror and formed into a light sheet using a cylindrical lens. The laser sheet subsequently illuminates different cross-sections of the flow field. Images are then acquired for each laser pulse and a 3-D image can be reconstructed from the image sequence. A brief description of each of these main components is given here.

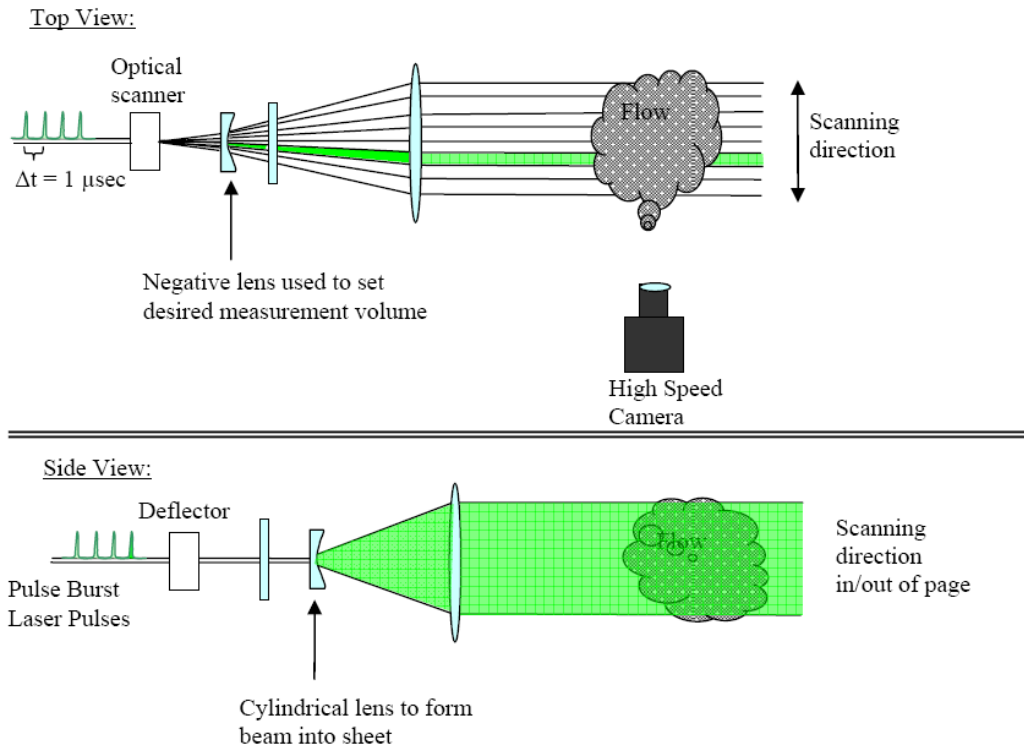


Figure 1 – Schematic of High-Speed 3-D Flow Visualization System

#### A. Pulse Burst Laser System

The AU pulse burst laser system is still under construction and was not available for the current work; however, a brief description of its design and working principles are provided here. A more in-depth discussion of the design of the AU pulse burst laser system can be found in Ref. [16].

The AU pulse burst laser system is a 3rd generation design based on similar systems described by Refs. [17] – [19]. The basic concept is the formation and amplification of a train of short-duration laser pulses. In the AU system, the pulses are created using a low-power (100 mW) cw Nd:YAG laser operating at 1.064 microns and an acousto-optic modulator (AOM), a device traditionally used in some Q-switched lasers. The AOM acts as a high-speed deflector and is used to form the desired pulses by cycling the deflection on and off very rapidly. Each pulse is ~20 nsec in duration and contains ~1 nJ of energy. Repetition rate is only limited by the AOM, which has a bandwidth of 100 MHz. The pulses are then passed through an amplifier chain consisting of three flashlamp pumped, Nd:YAG rod amplifiers. Faraday isolators are used to isolate each amplification stage and avoid parasitic oscillations. The amplifier system has been designed to provide a gain of  $10^7$  over a period of time lasting approximately 1 msec. Thus, a burst of pulses with pulse energies up to ~10 mJ/pulse can be produced with the current system. The amplified pulses can then undergo 2nd harmonic generation to 532 nm using a type II KTP non-linear crystal which has a demonstrated efficiency of 40-50 percent. It should be noted that the pulse energy can

be increased by more than an order of magnitude through the addition of more amplifiers and 3rd (355 nm) and 4th (266 nm) harmonic generation is also possible.

#### B. Scanning Mirror

High-speed scanning of laser pulses is achieved using a commercially available galvanometric scanning mirror (General Scanning Inc. VM500). A similar mirror was used in Ref. [14]. The mirror has a 6 mm clear aperture and is AR coated for 532 nm. The mirror's position ( $\pm 20^\circ$ ) is controlled by a  $\pm 3V$  command input and monitored using a built in encoder. Fig. 2 shows the mirror's response to a step command to change position from  $-13^\circ$  to  $+13^\circ$ . The random access time (i.e. time to move from position A to position B) is ~1 msec. For high-speed applications, the laser pulses will occur while the mirror is in motion. As each laser pulse is ~20 nsec in duration, the mirror's position and, therefore, the laser sheet's position is essentially fixed. The angular velocity exceeds 100,000 degrees/sec over a ~150  $\mu$ sec period. This velocity corresponds to a slew rate of ~18 resolvable spots per microsecond indicating that the mirror is fast enough to enable scan rates as high as 18 MHz. In addition, the motion of the mirror was found to be highly repeatable with no noticeable jitter in angular position from one scan to the next. More details on the scanning mirror and its characteristics can be found in Ref. [20].

In addition to the scanning mirror, an acousto-optic deflector (AOD) has also been tested for the current application and is described in Ref [21]. While demonstrating the speeds necessary for high-speed 3-D imaging, the AOD had a poor deflection efficiency ranging from 30 – 60% across the full

scan. One advantage to an AOD, however, is that the random access time is 1  $\mu$ sec. This would allow for a randomization of

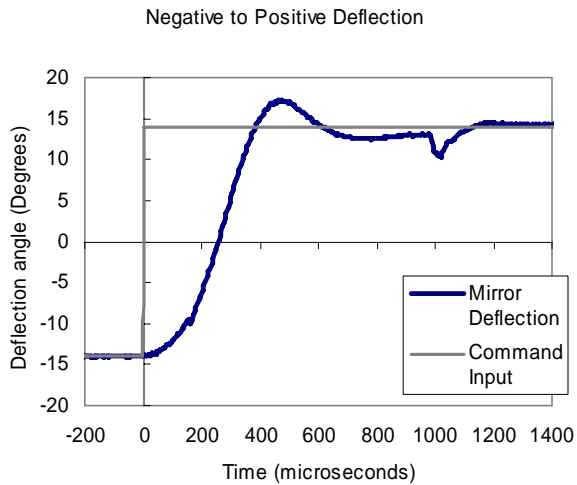


Figure 2 – Scanning mirror’s response to a step command input.

the scan and/or the ability to rapidly repeat the scan as might be required in a PIV type of application.

### C. High-Speed Cameras

Until recently, the number of ultra-high-speed cameras commercially available was quite scarce and a limiting factor for researchers trying to develop high-speed imaging technique. Fortunately, a large number of ultra-high speed cameras capable of framing rates on the order of 1 MHz are now commercially available. The characteristics of these cameras varies widely; Ref. [20] gives a brief review of currently available high-speed cameras.

In this work, we use a DRS Hadland Ultra68 for high-speed imaging. This camera utilizes multiple high-speed imaging methods to obtain 68 images with a resolution of  $\sim 240 \times 240$  pixels at up to 500,000 frames per second. It is also capable of burst framing rate of up to 100,000,000 frames per second in 4 frame bursts. Light entering the camera is directed along four different paths using a unique four-way beam splitter. Each image is then formed on one quadrant of the surface of a segmented intensifier, with the firing of each quadrant being independently controlled. The intensifier is attached to a masked CCD in which only one out of every 17 pixels is exposed to the incident light; the remaining pixels are masked and serve as on-chip charge storage bins. This allows the camera to be operated at higher frame rates than possible if each image were read out directly from the chip. Higher frame rates are achieved by synchronizing the exposure of the CCD with the intensifier resulting in a 68 frame sequence of images.

The beamsplitter, intensifier and CCD mask, which divides the signal and limits the fill factor, add a significant amount of noise to each of the images. The gain of the intensifier, however, is sufficient to overcome this noise with the camera

performing quite well in poorly illuminated conditions. For the current application, which is concerned with the imaging of smoke using a 200 mW 532 nm laser, the camera performed quite well. We found the contrast between the smoke and the background sufficient to visualize the unique flow patterns produced by the smoke, but, due to the magnitude of the image noise, would be hesitant to use it with techniques requiring more quantitative information about image intensity.

## III. LOW-SPEED DEMONSTRATION EXPERIMENTS

The ultimate goal of this work is to develop a high-speed 3-D flow visualization technique. Electrical problems in the flashlamp power supply, however, have delayed completion of construction of the pulse burst laser. As such, a low-speed version of the system was assembled using a 200 mW continuous-wave (cw) Nd:YAG laser in place of the pulse burst laser. Although this arrangement limited the maximum speed that could be obtained, it allowed us to move forward with the development of the system and gain experience until the pulse burst laser is completed, which should be shortly.

### A. Experimental Arrangement

For demonstration purposes, a small flow facility was constructed to produce interesting 3-D flow patterns and is pictured in Fig. 3. The facility consists of a box with a small hole ( $\sim 12$  mm diameter) cut out in the top. Incense is used to fill the box with smoke and slots located at the bottom of the box serve as an inlet for air to flow into the box. The heated air/smoke convects upwards and through the small hole, exhausting into a small test section for visualization. As the flow exhausts into the test section, large flow structures, such as mushroom vortices, quickly form producing a complex 3-D flow pattern. These structures were accentuated by manually disturbing the flow with periodic excitation (e.g. by flapping one’s hand near the inlet).

Fig. 4 shows a photograph of the 3-D flow visualization

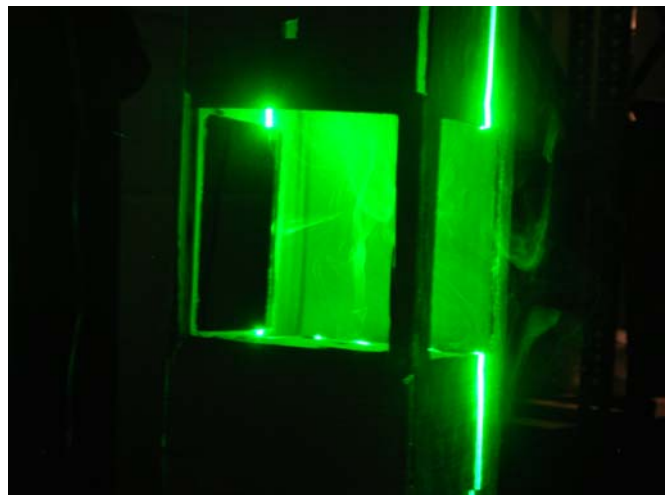


Figure 3 – Photograph of small flow facility with laser sheet illumination. Smoke chamber is beneath the illuminated smoke pattern.

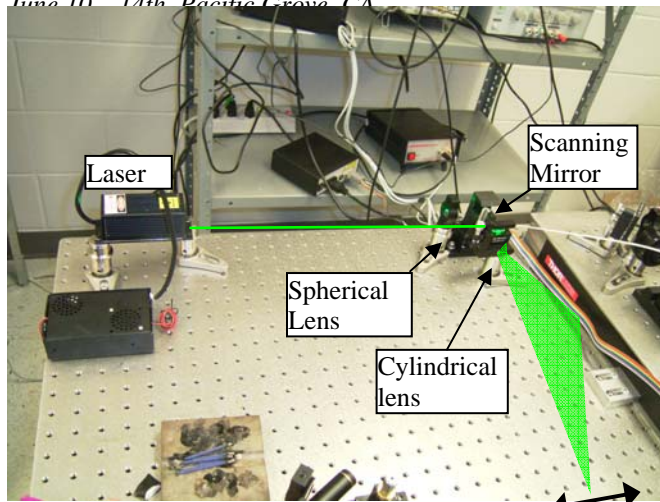


Figure 4 – Photograph of low-speed 3-D scanning system.

experimental arrangement. The laser is a 532 nm 200 mW diode pumped solid state Nd:YAG laser (Aixiz Lasers). The outputs reflects from a galvanometric scanning mirror at a nominal incidence angle of  $45^\circ$ . A +1,000 mm spherical lens and -25 mm cylindrical lens is used to form a laser sheet ( $\sim 1$  mm thick). A ramp signal is provided to the mirror causing it to rotate over a total deflection angle of  $\sim 5^\circ$  providing for a total scan distance of 85 mm with the flow facility located  $\sim 1$  m from the mirror.

The camera (DRS Ultra68) was located perpendicular to the laser sheet and outfitted with a 50 mm focal length lens with f/stop setting of 5.6, which was found to be sufficient to achieve good focus throughout the 3-D volume. A high f/stop is necessary to achieve a larger depth of focus consistent. The framing rate of the camera was set to 1,000 fps with an exposure time of 1 msec for each image. Labview was used to synchronize the camera with the movement of the laser sheet.



Figure 5 – 2-D image of flow field using a high-sensitivity, high-resolution camera.

68 images were acquired for each scan thus yielding a 3-D image exposure time of 68 msec. The imaged volume is approximately  $110 \times 110 \times 85$  mm ( $4.33'' \times 4.33'' \times 3.35''$ ) and the 3-D image resolution is  $220 \times 220 \times 68$  volumetric pixels (voxels). It should be noted that the voxels are deeper than they are wide due to the number of image frames used to cover the total scan depth.

### B. 2-D Flow Visualization

Fig. 5 shows a single 2-D image of the flow pattern obtained using a high sensitivity, high resolution camera (Cooke Corp Sencam QE,  $1376 \times 1024$  pixels resolution). The exposure time was 12 msec. The complex vortex pattern in the flow is quite clear and demonstrates the rich nature of the flow field. This particular image appears to indicate a train of counter-rotating (mushroom) vortices growing in the vertical direction and veering off slightly to the left. Fig. 6 shows a sequence of sixteen 2-D images (every 4<sup>th</sup> frame out of a sequence of 68 frames) obtained with the 3-D flow visualization system. It should be noted that each frame corresponds to a different 2-D plane within the 3-D test section volume separated by  $\sim 5$  mm each. Thus, any apparent motion is mainly due to the 3-D structure of the flow and not fluid motion, which is estimated to be below 1 m/s. The sequence of images shows some interesting 3-D features about the flow, such as how the size and location of vortices changes with depth.

### C. 3-D Flow Visualization

The true strength of the 3-D flow visualization experiments can be observed in the reconstructed 3-D images. The images were reconstructed in Matlab using, among others, the function **isosurface**. This function takes three-dimensional scalar data and computes a surface corresponding to a constant value within the 3-D data field. In this case, the value was image intensity with a numerical value of 75 (out of 255) chosen to produce the images in Figure 7. This threshold was above the background noise threshold of the images, but low enough to capture most of the observable flow structure. We are currently examining alternative methods for 3-D data visualization, such as that available in commercial software packages like Tecplot.

Fig. 7 shows a 3-D reconstruction formed using the image sequence shown in Fig. 6. Dimensions are given in pixels, however, the axes (i.e. scan direction) have been scaled to give a physically realistic picture of the flow. The reconstructed image clearly shows the 3-D structure associated with this flow. For example, the train of vortices appears to wrap around and originate from a point towards the front of the image. This could possibly be the result of a slight cross-flow (draft) in the room. In addition, a helical structure appears to have formed in the lower-front-right portion of the image. The break down of the vortices can be observed at the top of the image as indicated by the more chaotic structure. These types of features would be difficult to observe without this type of visualization.

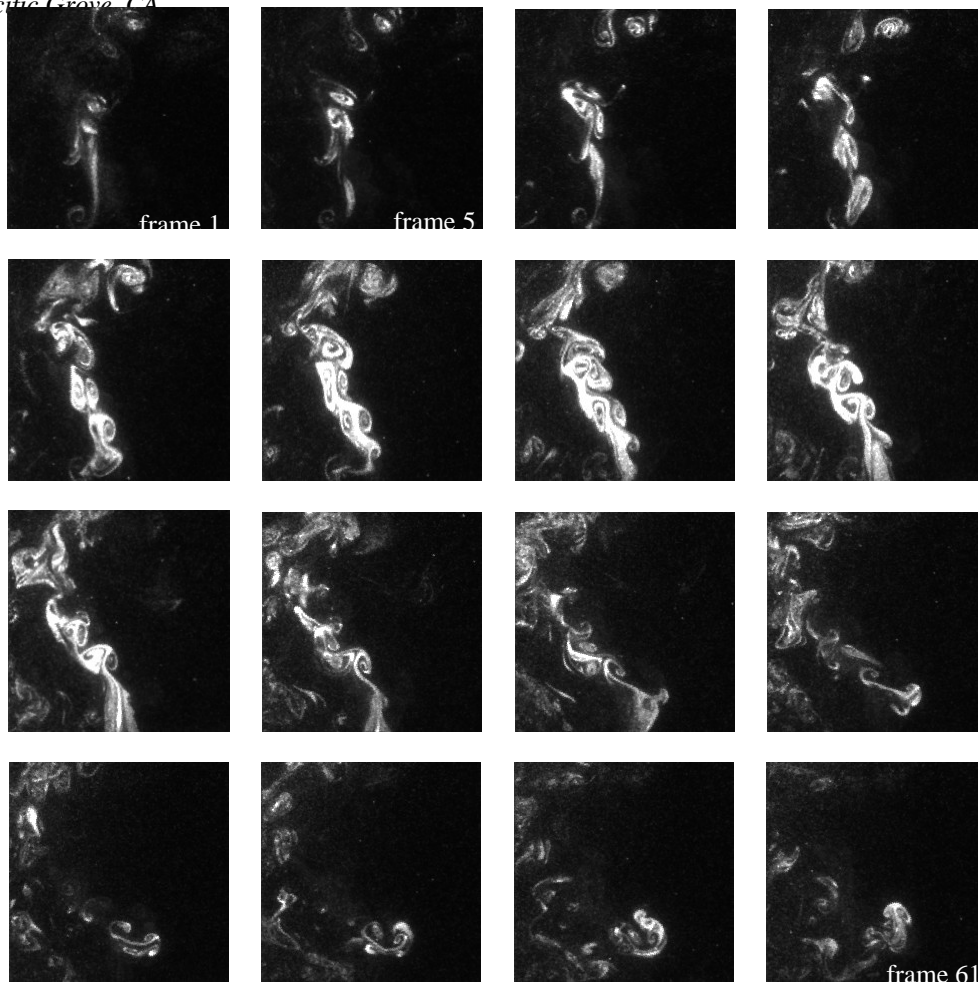


Figure 6 – Sequence of 16 (out of 68) images acquired with 3-D flow visualization system. Each image corresponds to a different 2-D plane of the flow field

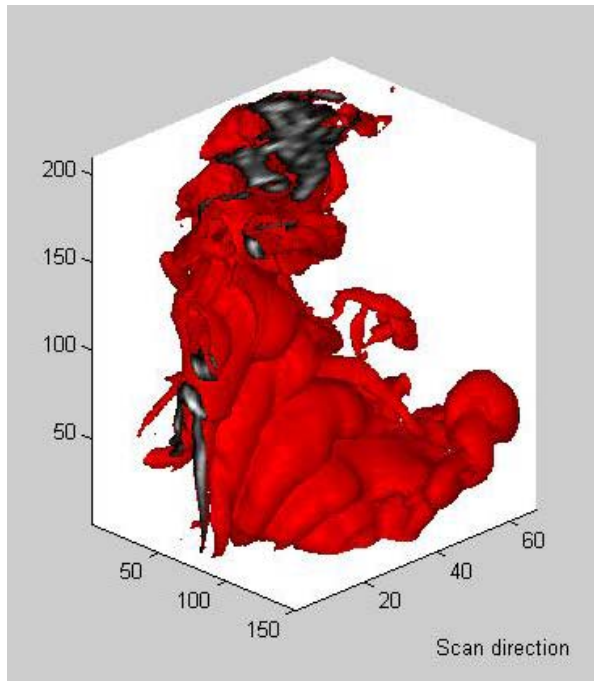


Figure 7 – 3-D reconstructions of images shown in Fig. 6.

Fig. 8 shows another example of a 3-D image. In this case, the flow takes the form of a helix as the smoke spirals upwards and spreads out in space. One difficulty with the current 3-D images is the inability to observe the internal structure of the flow. Interactive viewing of the images, which allows rotation, changed lighting, etc can reveal much more information about the flow. For example, Fig. 9 shows a cut through at about the midway point in the structure. In the upper part of the plum, a pair of counter-rotating vortices (mushroom like appearance) can be observed.

Figs. 10 and 11 are two more examples of the 3-D flow structure that can be observed with the technique described here. Fig. 10 appears to show the intertwining of elongated structures as the coherent vortices initially formed break down and transition into turbulence while Fig. 11 shows an interesting view on the influence of a cross-flow on the structures. Both images are of the same basic flow field, but show very different flow structures. The amount of information contained in these images is quite rich and reveal a tremendous amount of information that otherwise would be difficult to observe with traditional diagnostics.

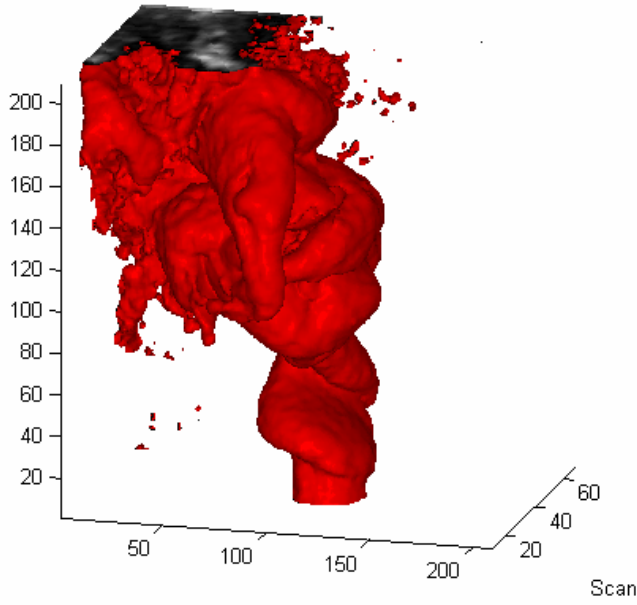


Figure 8 – 3-D image of helical structure.

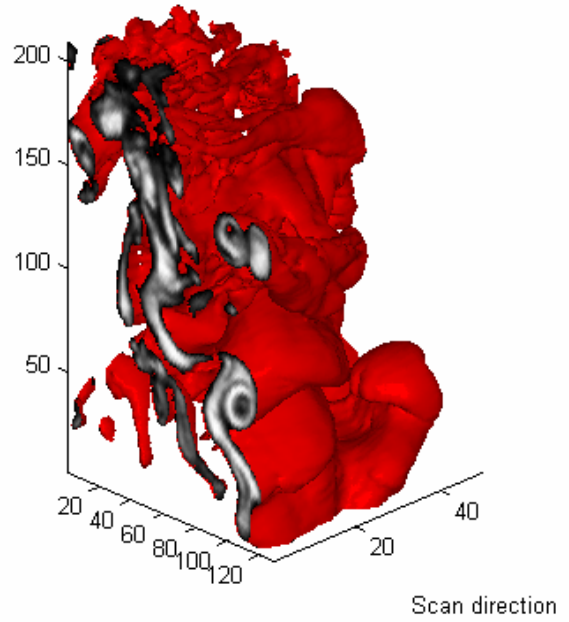


Figure 10 – 3-D image of entangled flow

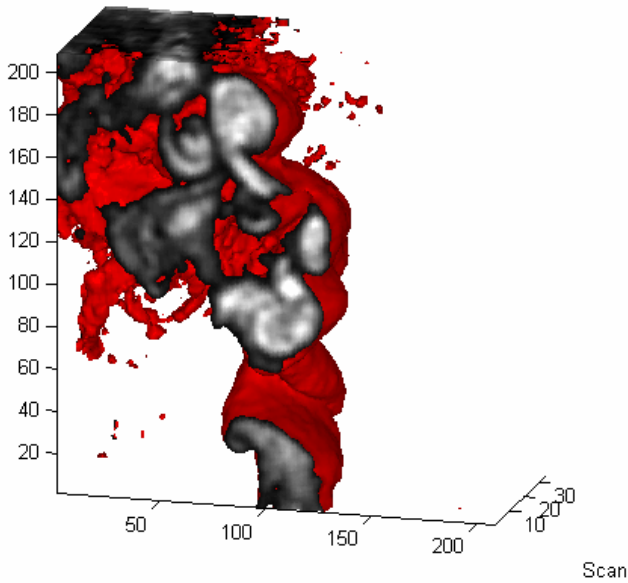


Figure 9 – Cut-away image of Fig. 8 showing internal structure of flow.

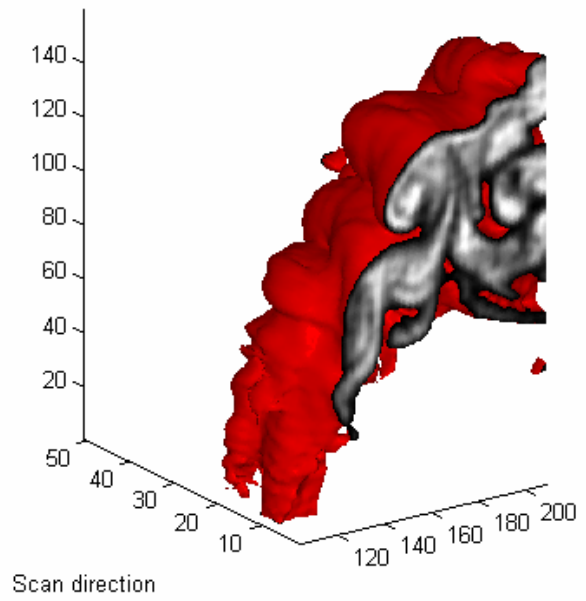


Figure 11 – 3-D image showing influence of cross-flow on structures.

#### IV. CONCLUSIONS AND FUTURE WORK

Significant progress has been made towards the development of a high-speed 3-D flow visualization system based on the rapid scanning and imaging of a laser sheet passing through the flow field. The system is based on a pulse burst laser system, a galvanometric scanning mirror and a high-speed camera. Once completed, the system will be able to acquire a 3-D image in the matter of 10s of microseconds, which is fast enough for a wide variety of flow fields, including some transonic and supersonic flow fields. The next step in development of this system is completing construction of the pulse burst laser system and incorporating it into the experimental arrangement to achieve these goals. It is estimated that the pulse burst laser will not only provide greater speed, but also better image quality as the pulse energy is 1-2 orders of magnitude greater than that used here.

The low-speed 3-D flow visualization system was set-up to demonstrate the potential of this technique and to gain experience with 3-D imaging in general. The 3-D flow visualization images shown here greatly demonstrate the potential of this technique to elucidate 3-D features that would not otherwise be apparent using conventional techniques. The images are quite rich in information and show complex vortex patterns. One difficulty encountered was in analyzing and displaying the large amount of information contained in these images. In addition, the current display does not correct for the change in the magnification across the imaging volume. An effort is currently under way to correct for this and to devise an appropriate calibration scheme so that this technique can be applied in a more controlled experimental setting.

#### ACKNOWLEDGMENT

The support of the Army Research Office (program manager: Dr. Thomas Doligalski) through the Young Investigator Program is gratefully acknowledged. The assistance of Aman Satija and Zhiguo Xu in setting up and conducting these experiments is appreciated.

#### REFERENCES

- [1] Guezennec, Y.G., Brodkey, R.S., Trigui, J. and Kent, J.C. "Algorithms for fully automated three-dimensional particle tracking velocimetry," *Exp. in Fluids*, Vol. 17, pp. 209-219, 1994.
- [2] Royer, H., "Holography and particle image velocimetry," *Meas. Sci. Technol.*, Vol. 8, pp. 1562-1572, 1997.
- [3] Trolinger, J.D., Rottenkolber, M. and Elandaloussi, F, *Meas. Sci. Technol.*, Vol. 8, pp. 1573-1583, 1997.
- [4] Sheng, J. Malkiel, E., and Katz, J., "Single beam two-views holographic particle image velocimetry," *App. Optics*, Vol. 42, pp. 235-250, 2003.
- [5] Elkins, C.J., Markl, M., Pelc., N. and Eaton, J.K., "4D Magnetic resonance velocimetry for mean velocity measurements in complex turbulent flows," *Exp. Fluids*, Vol. 34, pp. 494-503, 2003.

- [6] Kychakoff, G., Paul, P.H., Van Cruyningen, I. and Hanson, R.K., "Movies and 3-D Images of Flowfields Using Planar Laser-Induced Fluorescence," *App. Optics*, Vol. 26, pp. 2498-2500, 1987.
- [7] Long, M.B. and Yip, B., "Measurement of Three-Dimensional Concentrations in Turbulent Jets and Flames," *Proc. 21st Symp. on Comb.*, pp. 701-709, 1988.
- [8] Yip, B., Schmitt, R.L., and Long, M.B., "Instantaneous, Three-Dimensional Concentration Measurements in Turbulent Jets and Flames," *Opt. Letters*, Vol. 13, pp. 96-98, 1988.
- [9] Patrie, B.J., Seitzman, J.M., and Hanson, R.K., "Instantaneous Three-Dimensional Flow Visualization by Rapid Acquisition of Multiple Planar Flow Images," *Opt. Eng.*, vol. 33, pp. 975-980, 1994.
- [10] Goldstein, J.E. and Smits, A. J., "Flow Visualization of the Three-Dimensional, Time-Evolving Structure of a Turbulent Boundary Layer," *Phys. Fluids*, Vol. 6, pp. 577-587, 1994.
- [11] Island, T.C., Patrie, B.J., Mungal, M.G. and Hanson, R.K., "Instantaneous Three-Dimensional Flow Visualization of a Supersonic Mixing Layer," *Exp. Fluids*, Vol. 20, pp. 249-256, 1996.
- [12] Brucker, CH, "3D scanning PIV applied to an air flow in a motored engine using digital high-speed video," *Meas. Sci. Technol.*, Vol. 8, pp. 1480-1492, 1997.
- [13] Delo, C and Smits, A.J., "Volumetric Visualization of Coherent Structure in a Low Reynolds Number Turbulent Boundary Layer," *Int. J. of Fluid Dyn.*, Vol. 1, 1997.
- [14] Hult, J., Omrane, A., Nygren, J., Kaminski, C.F., Axelsson, B., Collin, R., Bengtsson, P.-E., and Alden, M., "Quantitative Three-Dimensional Imaging of Soot Volume Fraction in Turbulent Non-Premixed Flames," *Exp. Fluids*, Vol. 33, pp. 265-69, 2002.
- [15] Tian, X. and Roberts, P.J.W., "A 3D LIF System For Turbulent Buoyant Jet Flows," *Exp. Fluids*, Vol. 35, pp. 636-647, 2003. efficiency of 40-50 percent. Other harmonics are also available.
- [16] Thurow, B. and Satija, A., "Characteristics of a 10 MHz Repetition Rate Pulse Burst Laser System at Auburn University," *AIAA Paper 2006-1384*, 44th AIAA Aerospace Sciences Meeting and Exhibit, Reno, NV, 2006.
- [17] Lempert, W. R., Wu., P., Zhang, B., Miles, R. B., Lowrance, J. L., Mastracola, V., and Kosonocky, W. F., "Pulse-burst laser system for high speed flow diagnostics," *AIAA Paper 96-0179*, (1996).
- [18] Wu, P., Lempert, W. R., and Miles, R. B., "MHz pulse-burst laser system and visualization of shock-wave/boundary-layer interaction in a Mach 2.5 wind tunnel," *AIAA J.*, Vol. 38, 672, (2000).
- [19] Thurow, B., Jiang, N., Lempert, W. and Samimy, M., "A MHz Rate Pulse Burst Laser for High-Speed Flow Diagnostics," *Applied Optics*, Vol. 43, No. 26, pp. 5064-5073, September 2004.
- [20] Thurow, B. and Satija, A., "Preliminary Development of a Nearly-Instantaneous Three- Dimensional Imaging Technique for High-Speed Flow Fields," *AIAA Paper 2006-2972*, 25th Aerodynamic Measurement Technology and Ground Testing Conference, San Francisco, CA, June 2006.
- [21] Thurow, B., and Satija, A., "Further Development of a High-Speed Three-Dimensional Flow Visualization System," *AIAA Paper 2007-1060*, 45th AIAA Aerospace Sciences Meeting, Reno, NV, January 2007.